Testing the Froggatt-Nielsen mechanism with lepton flavor and number violating processes

Claudia Cornella,[1,*] David Curtin,[2,†] Gordan Krnjaic,[3,4,5,‡] and Micah Mellors[2,§]

[1]*Theoretical Physics Department, CERN, Geneva, Switzerland*
[2]*Department of Physics, University of Toronto, 60 St George St, Toronto, ON M5S 1A7, Canada*
[3]*Theoretical Physics Division, Fermi National Accelerator Laboratory, Batavia, Illinois, USA*
[4]*Department of Astronomy and Astrophysics, University of Chicago, Chicago, Illinois, USA*
[5]*Kavli Institute for Cosmological Physics, University of Chicago, Chicago, Illinois, USA*

(Received 10 February 2025; accepted 31 October 2025; published 3 December 2025)

The Froggatt-Nielsen (FN) mechanism offers an elegant explanation for the observed masses and mixings of Standard Model fermions. In this work, we systematically study FN models in the lepton sector, identifying a broad range of charge assignments ("textures") that naturally yield viable masses and mixings for various neutrino mass generation mechanisms. Using these textures, we consider higher-dimensional operators consistent with a FN origin and find that natural realizations predict distinct patterns in lepton flavor- and number-violating observables. For Dirac and Majorana neutrinos, FN-related correlations can lead to detectable rates of charged lepton flavor violation at next-generation low-energy experiments. Majorana and type-I seesaw models predict measurable rates of neutrinoless double beta decay. Determination of inverted neutrino mass ordering would exclude the Dirac neutrino FN scenario. Only a small minority of purely leptonic FN models predict detectable flavor violation at future muon colliders, though it is possible that a combined analysis with the quark sector will reveal motivated signals. These findings highlight the power of the FN mechanism to link neutrino mass generation to testable leptonic observables, offering new pathways for the experimental exploration of lepton number and underscoring the importance of next-generation low-energy probes.

DOI: 10.1103/c2ws-hx4h

I. INTRODUCTION

Standard Model (SM) fermions exhibit a broad range of masses and mixing angles with distinct patterns. While technically natural, this dramatic variation invites an explanation beyond the SM. The Froggatt-Nielsen (FN) mechanism [1] provides an elegant and economical framework for explaining this structure through a spontaneously broken horizontal symmetry.

In these models, fermions carry additional FN charge and Yukawa couplings are forbidden at tree level. At low energies, the new symmetry is spontaneously broken and heavy fields are integrated out, yielding effective Yukawa couplings whose magnitude is exponentially sensitive to the FN charges of the corresponding fermions. Thus, order one differences in charge assignments generate large hierarchies in masses and mixing parameters.

This mechanism has been studied in both the quark and lepton sectors [2–32]. The lepton sector, which is the focus of this work, introduces the additional challenge of integrating neutrinos into the framework. Unlike quarks, whose masses and mixings all arise from Dirac-like Yukawa couplings, the underlying mechanism for generating neutrino masses is currently unknown, leading to a greater variety of possible implementations. Furthermore, the Pontecorvo Maki Nakagawa Sakata (PMNS) matrix does not exhibit any hierarchies and there are large experimental uncertainties on the parameters of this sector; indeed, the precise values of neutrino masses are currently unknown.

In this work, we address these challenges systematically to present for the first time a *global* picture of the expected relative magnitudes of CLFV observables resulting from a large number of phenomenologically viable lepton FN textures. We also present the correlations between observables which could, in principle, be used to discriminate between textures. We achieve this through a two step procedure:

(1) *Identify realistic natural FN textures:* We first scan over a wide range of FN charge assignments

*Contact author: claudia.cornella@cern.ch
†Contact author: dcurtin@physics.utoronto.ca
‡Contact author: krnjaicg@fnal.gov
§Contact author: m.mellors@mail.utoronto.ca

("textures") for the leptons and identify hundreds of combinations that naturally yield viable lepton masses and mixings. In our treatment, all other parameters (e.g., the coefficients of FN-preserving operators) are chosen to be generic order-one numbers such that the hierarchies in the lepton sector arise entirely from the charge assignments and corresponding FN spurion insertions.

(2) *Predict CLFV and $0\nu\beta\beta$ for these textures:* Although the SM does not predict observable levels of charged lepton flavor violation (CLFV) or neutrinoless double beta decay ($0\nu\beta\beta$), such processes can be greatly enhanced in the presence of higher-dimensional operators that arise from integrating out the FN sector. The relative importance of different observable processes is dictated by texture-specific selection rules for each model. We therefore calculate the predicted rates of lepton-violating processes for the identified realistic textures within the Standard Model Effective Theory (SMEFT) framework, which allows us to *evaluate the experimental prospects of the leptonic FN mechanism as a whole*.

We consider neutrino mass generation by three mechanisms: Dirac, generic Majorana via a Weinberg operator, and type-I seesaw.[1] Our analysis reveals how a variety of low-energy, high-energy, and cosmological probes can provide a direct window into the dynamics underlying lepton flavor.

II. FROGGATT-NIELSEN NEUTRINO MASSES

The FN mechanism introduces a $U(1)_{\rm FN}$ symmetry which is spontaneously broken at a UV scale Λ by the vacuum expectation value (VEV) of a heavy scalar ϕ. $\epsilon \equiv \phi/\Lambda \ll 1$ is the spurion associated with the breaking of $U(1)_{\rm FN}$. Without loss of generality, we take the FN charge of ϕ (SM Higgs) to be $X_\phi = 1$ ($X_H = 0$), and the VEV of ϕ to be in the positive real direction. The SM Yukawa couplings only arise through ϵ insertions after FN breaking.

In two-component fermion notation, the charged lepton Yukawa couplings take the form

$$\mathcal{L}_Y \supset -c^{\ell}_{ij} L_i H^\dagger \bar{e}_j \epsilon^{|X_{L_i} + X_{\bar{e}_j}|}, \tag{1}$$

where L_i are the left-handed (LH) lepton doublets, e_j the right-handed (RH) charged lepton singlets, H the Higgs doublet, c^{ℓ} a coupling matrix with $\mathcal{O}(1)$ entries, and $i, j = 1, 2, 3$ label the fermion generations. The resulting Yukawa matrix is $(Y_\ell)_{ij} \equiv c^{\ell}_{ij}\epsilon^{n^{\ell}_{ij}}$, $n^{\ell}_{ij} \equiv |X_{L_i} + X_{\bar{e}_j}|$, naturally generating hierarchies when $\epsilon \ll 1$. Diagonalizing the Yukawas yields the charged lepton masses $Y_\ell = U_\ell \hat{Y}_\ell W^\dagger_\ell \Rightarrow \hat{m}_\ell = \frac{v}{\sqrt{2}}\hat{Y}_\ell$ after electroweak symmetry breaking (EWSB), where $\hat{Y}_\ell$ is diagonal, U_ℓ and W_ℓ are unitary, and $v = 246$ GeV. To account for neutrino masses, we examine three generation mechanisms within the FN framework.

Dirac: Here, the SM is supplemented with right-handed (RH) neutrinos N_i, and neutrino masses only arise from the Yukawa couplings

$$\mathcal{L}_D \supset c^{\nu}_{ij}\epsilon^{n^{\nu}_{ij}} H L_i N_j, \qquad n^{\nu}_{ij} \equiv |X_{L_i} + X_{N_j}|, \tag{2}$$

where c^ν is a matrix with order-one entries. In analogy with charged leptons, the neutrino Yukawa matrix can then be written as $(Y_\nu)_{ij} \equiv c^{\nu}_{ij}\epsilon^{n^{\nu}_{ij}}$ and yields $Y_\nu = U_\nu \hat{Y}_\nu W^\dagger_\nu \Rightarrow \hat{m}_\nu = \frac{v}{\sqrt{2}}\hat{Y}_\nu$, where $\hat{Y}_\nu$ is the diagonal Yukawa matrix, U_ν and W_ν are unitary matrices, $\hat{m}_\nu$ is the diagonal mass matrix, and the PMNS matrix can be written as $V \equiv U^\dagger_\ell U_\nu$.

In this scenario, the FN sector preserves lepton number, and the smallness of neutrino masses is entirely due to the FN mechanism and large flavor charges for RH neutrinos.

Majorana: The Weinberg operator [33]

$$\mathcal{L}_W \supset -\frac{c^W_{ij}\epsilon^{n^W_{ij}}}{\Lambda_W}(L_i H)(L_j H), \tag{3}$$

generates neutrino masses, where $n^W_{ij} \equiv |X_{Li} + X_{Lj}|$, c^W is a symmetric matrix with $\mathcal{O}(1)$ elements, and Λ_W is the effective scale at which the operator is generated, which generically differs from the FN scale Λ. After EWSB, Majorana neutrino masses arise via

$$\hat{m}_\nu = U^T_\nu \left[c^W \epsilon^{n^W} \frac{v^2}{\Lambda_W} \right] U_\nu, \tag{4}$$

where U_ν is a unitary matrix, $\hat{m}_\nu$ is the diagonalized mass matrix, and $V = U^\dagger_\ell U_\nu$ is the PMNS matrix.

Seesaw: We consider a type-I seesaw scenario [34–37] where flavor breaking and lepton violation are governed by the FN mechanism. In this case, neutrinos receive both Dirac and Majorana mass terms,

$$\mathcal{L}_{\rm SS} \supset -c^{\nu}_{ij}\epsilon^{n^{\nu}_{ij}} H L_i N_j - c^M_{ij}\epsilon^{n^M_{ij}} \frac{M}{2} N_i N_j, \tag{5}$$

where c^ν and c^M are matrices of order-one coefficients, M is the Majorana mass scale of the RH neutrinos, and $n^{\nu}_{ij} \equiv |X_{L_i} + X_{N_j}|$, $n^M_{ij} \equiv |X_{N_i} + X_{N_j}|$. In the seesaw limit, the Dirac contribution is small and the diagonal neutrino mass matrix is

[1]Note that while many type-I seesaw scenarios can be mapped directly to a Weinberg operator with a single Weinberg scale, as in the Majorana case, if the RH neutrinos have flavor charge, the type-I seesaw would effectively generate a Weinberg operator where the suppression scale has flavor structure.

$$\hat{m}_\nu \approx \frac{v^2}{2M} U_\nu^T (c^\nu \epsilon^{n^\nu})(c^M \epsilon^{n^M})^{-1} (c^\nu \epsilon^{n^\nu})^T U_\nu, \tag{6}$$

where U_ν is a unitary rotation matrix. It is natural to identify the FN scale with the Majorana mass scale ($M = \Lambda$). There could also be additional explicit lepton number violation in the FN sector, but we find that this yields qualitatively similar results, see Supplemental Material [38]. Note that type-I seesaw models generate an effective Weinberg operator through RH neutrino exchange, which ultimately gives rise to active neutrino masses. However, as the RH neutrino masses are also set by the FN mechanism, the resulting effective Λ_W carries strong flavor dependence, distinguishing this scenario from the minimal Majorana scenario introduced previously.

Note that most explicit models of neutrino mass generation can be accommodated within these scenarios [62–66], see Supplemental Material [38].

III. METHODS

Identifying Realistic Natural FN Textures: We begin by identifying viable FN textures that adequately reproduce the observed lepton masses and mixing parameters for a common value of ϵ. To ensure that, for a given texture, all hierarchical structure arises only from ϵ, we demand that all other free parameters are order-one numbers. In our analysis, these free parameters are encoded in the Lagrangian coefficients $c_{ij}^\ell, c_{ij}^\nu, c_{ij}^W$, and c_{ij}^M from Eqs. (1)–(3), and (5), respectively. We scan over a wide range of possible FN charges and determine the fraction of random $\mathcal{O}(1)$ values in these coefficients that reproduce all observed masses and mixings within some tolerance.

Our scanning procedure avoids conducting direct fits to the experimental observables. Instead, we seek to exhaustively identify charge assignments that resemble our world over a majority of their natural parameter space, realizing the intended spirit of a *natural* FN solution to the flavor problem. Thus, our predictions are derived for FN models which generate experimental predictions very close to their observed values, though the fit is not exact. However, we have confirmed that, for coefficients that approximately reproduce known results, introducing small post-hoc tweaks readily accommodates all known observables exactly. Thus, our scanning strategy does not lose any essential generality by seeking out approximate fits to experimental data.

Specifically, we adopt and extend the Bayesian-inspired method of Ref. [30] to the lepton sector—see Supplemental Material [38] for details. For each mass generation mechanism, we consider all textures with charges $|X| \leq 7$, and, for Dirac RH neutrinos, $|X| \leq 9$ as required to obtain viable models. For each texture, we generate random coefficient matrices c_{ij}, with each $\log_{10} c_{ij}$ sampled from a normal distribution centered on zero with standard deviation $\sigma = 0.3$, and phases sampled uniformly over $[0, 2\pi]$. (Alternative choices of reasonable "$\mathcal{O}(1)$" priors do not meaningfully affect results.)

For each choice of coefficients, we compute observables $\mathcal{O} = \{m_\ell, \Delta m_{ij}^2, |V_{ij}|, \sum m_\nu\}$, corresponding to the charged lepton masses, neutrino mass-squared differences, the absolute value of the PMNS matrix elements, and the sum of neutrino masses. The fractional deviation of each FN prediction $\mathcal{O}_{\rm FN}$ is $\delta_\mathcal{O} \sim \mathcal{O}_{\rm FN}/\mathcal{O}_{\rm exp}$, where $\mathcal{O}_{\rm exp}$ is the experimentally measured value, see Supplemental Material [38]. We maximize over all observables to obtain the overall experimental deviation: $\delta_{\rm max} \equiv \max_\mathcal{O}(\delta_\mathcal{O})$. Next, we adjust ϵ and, where applicable, Λ_W or Λ, to minimize $\delta_{\rm max}$. For each texture, this process is repeated many times for many choices of order-one coefficients. Textures that naturally resemble our world will have $\delta_{\rm max} \sim \mathcal{O}(1)$ for large fraction coefficient choices. To compare textures, we define $\mathcal{F}_x \equiv$ % of coeff. choices for which $\delta_{\rm max} \leq x$, allowing for textures to be ranked by $\mathcal{F}_x$ for different x.

In the Dirac case, leptonic masses and mixings depend only on ϵ, so the procedure outlined above leaves Λ unconstrained. For the Majorana (type-I seesaw) scenario, neutrino masses and mixings explicitly depend on both ϵ and Λ_W (Λ), constraining both when minimizing $\delta_{\rm max}$.

Predicting Lepton Violation in FN: Having identified the realistic and natural textures capable of reproducing leptonic masses and mixings, we next explore their implications for current and future experiments with a focus on lepton flavor violation. To remain agnostic about the UV completion of the FN mechanism, we adopt the SMEFT framework with the minimal assumption that ϵ is the only spurion of $U(1)_{\rm FN}$ breaking. Assuming $\mathcal{O}(1)$ coefficients in the UV theory, higher-dimensional SMEFT operators are then suppressed only by powers of Λ and insertions of ϵ.

The most relevant interactions for LFV processes are the four-lepton, dipole, and semileptonic operators. The four-lepton terms are

$$\mathcal{O}_4 = \frac{c_{ijkl}}{\Lambda^2} (\bar{\psi}_i \psi_j)(\bar{\psi}_k \psi_l) \epsilon^{n_{ijkl}}, \tag{7}$$

where c_{ijkl} are $\mathcal{O}(1)$ coefficients and we have defined $n_{ijkl} \equiv |X_{\psi_i} - X_{\psi_j} + X_{\psi_k} - X_{\psi_l}|$. Note that we switched to four-component fermion notation to match SMEFT conventions, but we write n_{ijkl} in terms of the FN charges of the corresponding two-component fermion fields. For dipole operators, we have

$$\mathcal{O}_d = \frac{c_{ij}}{\Lambda^2} (\bar{L}_i \sigma^{\mu\nu} e_j) H F_{\mu\nu} \epsilon^{n_{ij}}, \qquad n_{ij} \equiv |X_{L_i} + X_{\bar{e}_j}|, \tag{8}$$

where $F_{\mu\nu}$ is the field strength tensor of an electroweak gauge boson. Rates for muon to electron conversion in atomic nuclei are also sensitive to semileptonic four-fermion operators of the form Eq. (7), with one of the bilinears comprised of light quark fields (u, d, s). To be

agnostic to the flavor structure of the quark sector, we include only the flavor diagonal quark operators. Notably, the structure of these operators is such that textures with a nonzero Higgs charge can be mapped onto $X_H = 0$ textures without altering the phenomenology, as discussed in the Supplemental Material [38].

In our analysis, $\mathcal{O}(1)$ Wilson coefficients are generated on the FN basis at a high scale Λ and subsequently rotated into the mass basis using the values of ϵ and the U and W matrices from Eqs. (4), (6), built using the Lagrangian coefficients appropriate to each scenario. We calculate low-energy observables, including two- and three-body CLFV decays of muons and taus, as well as muon-to-electron conversion in nuclei using the FLAVIO package [67]. Matching to the relevant energy scales is performed with WILSON [68] (running was found to be a negligible effect). Based on experimental constraints, we derive lower bounds on Λ. Finally, using these bounds, we estimate the highest possible rates of $e\mu$, $e\tau$, and $\mu\tau$ production at future e^+e^- and $\mu^+\mu^-$ colliders. For comparison, we also compute the predictions for a fully anarchic or *null* texture, where all charges are set to zero and the Wilson coefficients are assumed to be all $\mathcal{O}(1)$ at a fixed scale. Further details on our methodology can be found in the Supplemental Material [38].

IV. RESULTS

The top-ranked textures for each mass-generation mechanism are presented in Table I—additional textures are provided in the Supplemental Material [38]. For both the Dirac and Majorana cases, the hierarchical structure of the charged lepton masses primarily stems from the charges of the RH charged leptons, and this fact has significant phenomenological implications. In particular, the LH rotation matrices often feature large off-diagonal terms, leading to relatively uniform contributions to various LFV processes across different textures and ultimately making the FN mechanism more predictive. Purely leptonic FN models of any type only rarely generate observable flavor-violating signals at proposed muon colliders; see Supplemental Material for details [38].

CLFV Dirac: In most Dirac FN models, the FN scale is constrained to satisfy $\Lambda \gtrsim 10^6$ GeV by limits on $\mu \to e\gamma$ [69] or muon conversion in Gold [70]—see the Supplemental Material [38] for details. Setting Λ to saturate its constraint within each individual model determines the highest possible rates for future CLFV signals. As shown in Fig. 1, Dirac FN textures can then predict measurable signals in LFV muon decays and μ-e conversion in atomic nuclei. The latter will be probed in new experiments with aluminum targets [71] (though gold targets would provide the greatest discriminatory power between textures). Furthermore, stringent constraints in the muon sector lead to suppressed LFV τ decays, with only a few textures approaching detectability in τ-related channels. Overall, the predicted signal rates for FN Dirac scenarios typically exceed those of anarchic models by more than an order of magnitude, particularly for muonic processes, and offer a modest degree of discriminatory power between different textures.

Majorana: Results depend on whether the Weinberg operator scale Λ_W coincides with the FN scale Λ. If $\Lambda_W = \Lambda$, the predictions for CLFV processes are fixed by neutrino masses, see Fig. 2 (top). In this scenario, a non-observation in future experiments would exclude specific textures entirely. Unfortunately, most of the top Majorana textures correspond to scales $\Lambda_W \sim 10^8$–10^{15} GeV, far beyond the reach of current or planned experiments. A handful of textures approach the observable region, exclusively in LFV muon experiments. The assumption $\Lambda_W = \Lambda$ can be relaxed, as in FN type-II seesaw models. If we instead let Λ saturate the most constraining current bounds, as in

TABLE I. Some of the most natural and realistic FN textures for Dirac, Majorana, and type-I seesaw neutrinos, reproducing masses and mixings with a relative experimental deviation factor $\delta_{\max} < 5$, 2, and 1.35 for approximately 50%, 2–5%, and 0.03% of random $\mathcal{O}(1)$ coefficient choices, respectively. Each texture is specified by the FN charges of the LH lepton doublets (X_{L_i}), RH charged leptons ($X_{\bar{e}_i}$), and RH neutrinos (X_{N_i}). For ϵ and $\log_{10}(\Lambda/\text{GeV})$, we show texture-averages for coefficient choices with $\delta_{\max} < 2$. NO denotes the percentage of coefficient choices that predict normal ordered (NO) neutrino masses.

Dirac											Majorana									Type-I seesaw										
L_1	L_2	L_3	$\bar{e}_1$	$\bar{e}_2$	$\bar{e}_3$	N_1	N_2	N_3	ϵ	NO	L_1	L_2	L_3	$\bar{e}_1$	$\bar{e}_2$	$\bar{e}_3$	ϵ	$\log\Lambda$	NO	L_1	L_2	L_3	$\bar{e}_1$	$\bar{e}_2$	$\bar{e}_3$	N_1	N_2	N_3	ϵ	$\log\Lambda$	NO
6	5	5	−3	−2	0	9	8	8	0.10	96	2	0	−1	7	6	4	0.24	15	91	6	1	−1	7	7	6	3	0	−4	0.36	14	93
3	3	3	2	−1	−6	9	9	8	0.07	99	5	5	−2	7	−2	−3	0.08	12	3	6	1	−1	6	6	6	3	0	−4	0.34	14	93
3	3	3	2	−5	−6	9	9	8	0.07	99	4	4	3	5	2	0	0.23	11	96	6	1	−2	7	7	7	5	0	−4	0.37	14	93
7	7	6	−4	−2	0	9	9	9	0.14	99	7	6	5	7	3	0	0.39	11	97	7	2	−1	7	7	7	4	0	−5	0.40	14	95
7	7	6	−4	−3	−1	9	7	7	0.11	99	6	6	5	5	1	−1	0.30	10	96	6	2	−6	2	1	1	3	2	−4	0.16	12	90
3	3	3	2	0	−5	9	9	8	0.07	99	7	7	6	2	−1	−3	0.23	7.6	96	4	1	−1	6	5	5	6	0	−3	0.27	14	93
3	3	3	2	0	−1	9	9	8	0.07	99	5	5	4	6	2	0	0.30	11	96	4	1	−1	7	5	5	4	0	−3	0.29	14	93
6	5	5	−3	−2	0	9	7	7	0.08	97	7	7	6	4	0	−2	0.30	9	96	7	2	−1	7	7	6	4	0	−5	0.39	14	95
7	3	3	2	0	−5	9	9	9	0.08	93	5	5	−2	7	−2	−7	0.08	12	3	6	1	−1	7	6	6	3	0	−4	0.35	14	93
6	6	6	−4	−3	−1	9	6	5	0.07	99	1	1	−1	−7	−5	−4	0.18	15	2	5	1	−1	5	5	5	2	0	−3	0.27	14	79

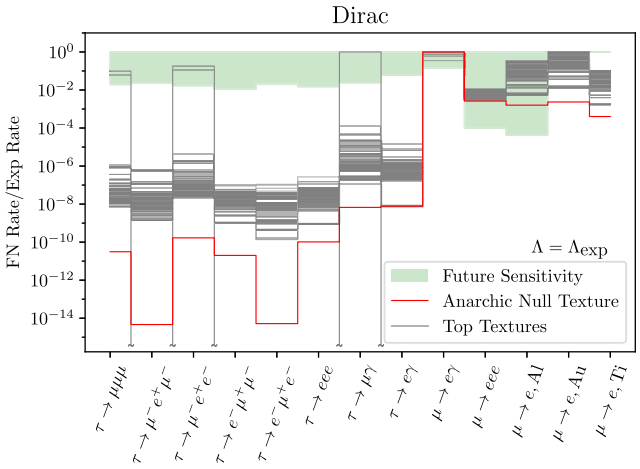

FIG. 1. Average predicted CLFV decay rates for the 100 most realistic natural Dirac FN textures (gray lines), relative to each observable's current constraint. In each model, the flavor scale was chosen to saturate current experimental bounds at $\Lambda \sim 10^6$ GeV, thus fixing the other rates. Green shading indicates the reach of proposed future low-energy CLFV experiments, and the flavor-anarchic null texture is shown as a red line for comparison.

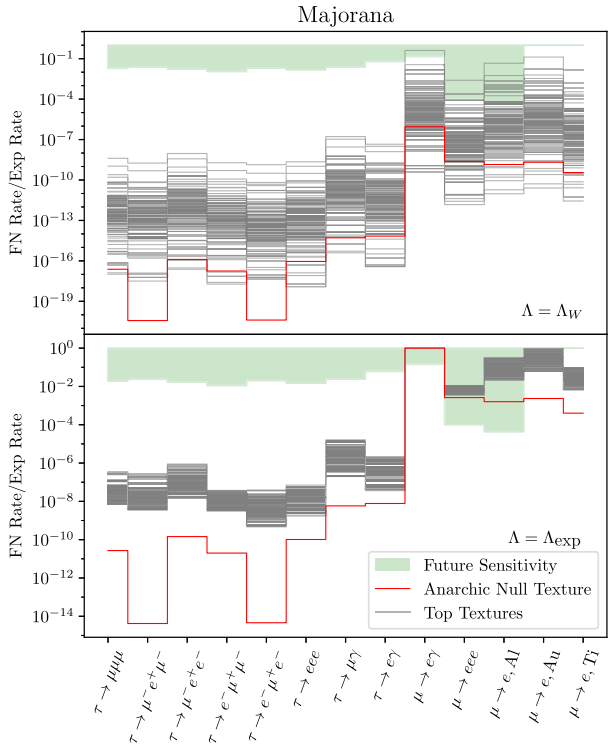

FIG. 2. Average predicted CLFV decay rates for the top 100 most realistic Majorana FN textures (gray lines), as in Fig. 1. The top panel assumes that the scale of the Weinberg operator (Λ_W) coincides with the FN scale (Λ), fixing the predictions for CLFV signals from the imposed neutrino mass constraints. The predicted neutrino scale for the null texture is set to 10^{14} GeV. The bottom panel assumes $\Lambda_W \neq \Lambda$, such as in FN type-II seesaw scenarios, where Λ is instead chosen to saturate its most restrictive current experimental bound of $\Lambda \sim 10^6$ GeV.

Fig. 1, it leads to the predictions shown in Fig. 2 (bottom). Majorana FN models then lead to similar, though slightly tighter, predictions in μ-e conversion experiments relative to the Dirac case.

Type-I Seesaw: These are the most challenging scenarios to probe experimentally. All observables are governed by the scale Λ, which is fixed by the scale of neutrino masses and is too high to predict observable signals at future experiments for our best textures, with a small number of exceptions, see Supplemental Material [38]. However, FN type-I seesaw scenarios can be probed more effectively via $0\nu\beta\beta$ decay experiments.

Additional information can be gained from correlations among lepton-violating observables, beyond their average predictions. For example, Fig. 4 shows how $\mathrm{BR}(\mu \to 3e)$ and $\mathrm{CR}(\mu \to e, \mathrm{Al})$ are correlated differently for two representative FN Dirac textures. These textures were chosen because they predict very similar *average* values for both observables, but their widely diverging distributions make it possible for two measurements to discriminate between these possibilities. Further correlation plots are included in the Supplemental Material [38].

Neutrino Mass Ordering: Most realistic natural textures in all scenarios favor normal ordering (NO). Inverted ordering (IO) is preferred by only a small fraction of Majorana textures and a somewhat larger subset of seesaw textures. Within the FN framework, an experimental determination of IO, e.g., by DESI measuring $\sum m_\nu$ with a precision of 0.02 eV [72], would therefore strongly disfavor Dirac neutrinos, while still allowing for Majorana or type-I seesaw scenarios.

$0\nu\beta\beta$ Decay: Predictions for $0\nu\beta\beta$ for 100 of the most realistic natural textures in Majorana and type-I seesaw models are shown in Fig. 3. For both scenarios, textures with IO consistently feature values of $m_{ee} = |\sum_i m_i V_{ei}^2|$ at the very lower edge of the currently allowed range. We emphasize that this is not imposed on our scan and constitutes a genuine prediction of the FN mechanism: while all shown analyses impose the cosmological bound on $\sum m_\nu$ [73], there are no meaningful changes if we instead impose the larger laboratory bound [74]. This IO prediction lies well within the capabilities of next-generation $0\nu\beta\beta$ experiments. For textures yielding NO, there are significant phenomenological differences between FN Majorana and type-I seesaw. The latter remains unlikely to be detected in upcoming laboratory searches—barring a few exceptional textures—while normal-ordered FN Majorana scenarios predict m_{ee} to lie well within or at most one order of magnitude below the sensitivity of upcoming laboratory searches. This opens up the tantalizing prospect of either detecting $0\nu\beta\beta$ or strongly disfavoring the entire Majorana FN framework.

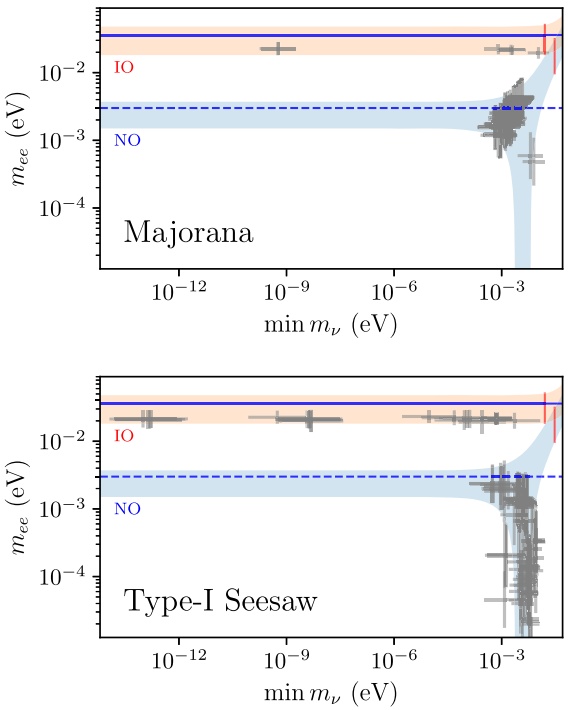

FIG. 3. Effective Majorana mass m_{ee} versus the mass of the lightest neutrino for the top 100 FN textures in the Majorana (top) and type-I seesaw (bottom) scenarios. The yellow- and blue-shaded regions indicate the allowed ranges for IO and NO, respectively, based on the current measured values for Δm^2_{32} and Δm^2_{21}. The solid blue line indicates the strongest exclusion from current $0\nu\beta\beta$ searches, from KamLAND-Zen [73], while the dashed blue line marks the reach of the future $0\nu\beta\beta$ experiments nEXO [75] and CUPID [76]. The vertical red lines indicate the limits on $\min m_\nu$ in the IO and NO scenarios from current cosmological limits on $\sum m_\nu$. Error bars show the 1σ spread of predictions with $\delta_{\max} < 2$.

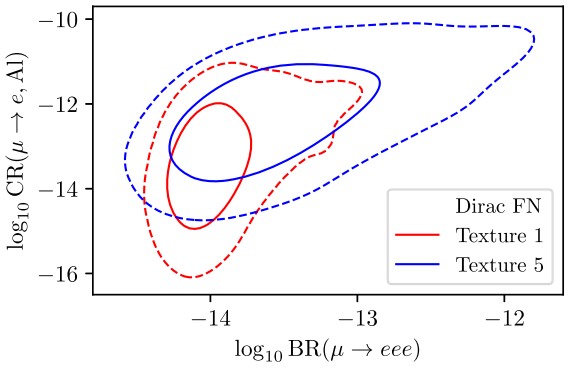

FIG. 4. Comparison of the predicted branching ratio for $\mu \to 3e$ and the conversion rate for μ-e conversion in Al for the first and fifth Dirac FN textures in Table I, assuming the FN scale Λ saturates its current lower bound. The conversion rate is normalized to the muon capture rate in nuclei. Contours show areas containing 68% (solid) and 98% (dashed) of random coefficient choices with $\delta_{\max} < 2$. Thus, these textures might be distinguished despite similar average predictions.

V. CONCLUSIONS AND OUTLOOK

In this work, we have systematically explored FN models in the leptonic sector, identifying realistic natural textures for Dirac, Majorana, and type-I seesaw neutrino mass generation mechanisms. Our study also sheds light on related scenarios, including type-II seesaw cases, see Supplemental Material [38]. By extending the FN framework to leptons, we demonstrated that Dirac and Majorana FN models predict distinct correlations in detectable CLFV rates, providing characteristic signatures that set them apart from anarchic scenarios. Experimental signals are most likely to appear in the muon sector, with $\mu \to e\gamma$, $\mu \to 3e$, and μ-e conversion on nuclei as the most promising channels for future probes. Our results also motivate new conversion experiments in a variety of targets, most notably gold in addition to the already planned aluminum [71]. FN models with Majorana and type-I seesaw neutrinos offer testable predictions for $0\nu\beta\beta$ decay experiments, and a determination of inverted neutrino mass ordering would disfavor Dirac FN models. Our conclusions are unaffected by adopting either cosmological or laboratory bounds on $\sum m_\nu$.

Our analysis constitutes the most model-exhaustive study of the Froggatt-Nielsen mechanism in the lepton sector to date, demonstrating both their universal predictive power and their capacity to diagnose the physics underlying lepton flavor. We anticipate that detection prospects will be greatly enhanced by considering observables involving flavor violation in both quarks and leptons, which motivates a joint analysis of the FN mechanism in both the quark and lepton sectors simultaneously. Integrating FN models with extended scalar sectors, such as multi-Higgs models, may also yield novel phenomenological insights in our model-exhaustive approach.

Note added. While this paper was being finalized, Ref. [32] appeared, which takes a more literally Bayesian method to identify realistic and natural FN charge assignments for quark and lepton sectors. This analysis adopts a broadly similar approach to our work, including considering both Majorana and type-I seesaw models. Their work includes larger maximum flavor charges and considers FN in both the quark and lepton sector, which allows them to consider nucleon decay observables. On the other hand, our lepton sector FN analysis is more general in the range of allowed ϵ values, nonzero flavor charges for RH neutrinos, the inclusion of the Dirac neutrino case, and our predictions for CLFV observables. Our analyses are therefore highly complementary.

ACKNOWLEDGMENTS

The work of C. C. was partially supported by the Cluster of Excellence *Precision Physics, Fundamental*

Interactions, and Structure of Matter (PRISMA$^+$, EXC 2118/1) within the German Excellence Strategy (Project-ID 390831469). C. C. would also like to thank Perimeter Institute for hospitality during the completion of this work. This research was supported in part by Perimeter Institute for Theoretical Physics. Research at Perimeter Institute is supported by the Government of Canada through the Department of Innovation, Science and Economic Development and by the Province of Ontario through the Ministry of Research, Innovation and Science. The work of D. C. and M. M. was supported in part by Discovery Grants from the Natural Sciences and Engineering Research Council of Canada (NSERC), the Canada Research Chair program, the Alfred P. Sloan Foundation, the Ontario Early Researcher Award, and the University of Toronto McLean Award. The work of M. M. was also supported in part by the NSERC Postgraduate Scholarship-Doctoral. Fermilab is operated by the Fermi Research Alliance, LLC under Contract DE-AC02-07CH11359 with the U.S. Department of Energy. This material is based partly on support from the Kavli Institute for Cosmological Physics at the University of Chicago through an endowment from the Kavli Foundation and its founder, Fred Kavli.

DATA AVAILABILITY

The data that support the findings of this article are openly available [77], embargo periods may apply.

[1] C. Froggatt and H. Nielsen, Hierarchy of quark masses, Cabibbo angles and *CP* violation, Nucl. Phys. **B147**, 277 (1979).
[2] M. Leurer, Y. Nir, and N. Seiberg, Mass matrix models, Nucl. Phys. **B398**, 319 (1993).
[3] M. Leurer, Y. Nir, and N. Seiberg, Mass matrix models: The sequel, Nucl. Phys. **B420**, 468 (1994).
[4] E. Dudas, C. Grojean, S. Pokorski, and C. A. Savoy, Abelian flavour symmetries in supersymmetric models, Nucl. Phys. **B481**, 85 (1996).
[5] N. Irges, S. Lavignac, and P. Ramond, Predictions from an anomalous U(1) model of Yukawa hierarchies, Phys. Rev. D **58**, 035003 (1998).
[6] J. Sato and K. Tobe, Neutrino masses and lepton flavor violation in supersymmetric models with lopsided Froggatt-Nielsen charges, Phys. Rev. D **63**, 116010 (2001).
[7] J. Sato and T. Yanagida, Low-energy predictions of lopsided family charges, Phys. Lett. B **493**, 356 (2000).
[8] D. Suematsu, The Origin of quark and lepton mixings, Phys. Rev. D **64**, 073013 (2001).
[9] H. K. Dreiner and M. Thormeier, Supersymmetric Froggatt-Nielsen models with baryon and lepton number violation, Phys. Rev. D **69**, 053002 (2004).
[10] Y. Nir and Y. Shadmi, The Importance of being majorana: Neutrinos versus charged fermions in flavor models, J. High Energy Phys. 11 (2004) 055.
[11] H. Kamikado, T. Shindou, and E. Takasugi, Froggatt-Nielsen hierarchy and the neutrino mass matrix, arXiv:0805.1338.
[12] F. Plentinger, G. Seidl, and W. Winter, Group space scan of flavor symmetries for nearly tribimaximal lepton mixing, J. High Energy Phys. 04 (2008) 077.
[13] W. Buchmuller, V. Domcke, and K. Schmitz, Predicting $\Theta_1 3$ and the neutrino mass scale from quark lepton mass hierarchies, J. High Energy Phys. 03 (2012) 008.
[14] S. Krippendorf, S. Schafer-Nameki, and J.-M. Wong, Froggatt-Nielsen meets Mordell-Weil: A phenomenological survey of Global F-theory GUTs with U(1)s, J. High Energy Phys. 11 (2015) 008.
[15] M. Bauer, T. Schell, and T. Plehn, Hunting the flavon, Phys. Rev. D **94**, 056003 (2016).
[16] Y. Ema, K. Hamaguchi, T. Moroi, and K. Nakayama, Flaxion: A minimal extension to solve puzzles in the standard model, J. High Energy Phys. 01 (2017) 096.
[17] L. Calibbi, F. Goertz, D. Redigolo, R. Ziegler, and J. Zupan, Minimal axion model from flavor, Phys. Rev. D **95**, 095009 (2017).
[18] K. Nishiwaki, Y. Shimizu, and Y. Tatsuta, Double Froggatt–Nielsen mechanism, Prog. Theor. Exp. Phys. **2016**, 083B05 (2016).
[19] V. V. Vien, H. N. Long, and A. E. Cárcamo Hernández, Fermion mass and mixing in a low-scale Seesaw model based on the S_4 flavor symmetry, Prog. Theor. Exp. Phys. **2019**, 113B04 (2019).
[20] F. Feruglio and A. Romanino, Lepton flavour symmetries, Rev. Mod. Phys. **93**, 015007 (2021).
[21] M. S. Berger and M. Dawid, A Froggatt–Nielsen flavor model for neutrino physics, Int. J. Mod. Phys. A **34**, 1950102 (2019).
[22] M. Bordone, O. Catà, and T. Feldmann, Effective theory approach to new physics with flavour: General framework and a leptoquark example, J. High Energy Phys. 01 (2020) 067.
[23] A. Smolkovič, M. Tammaro, and J. Zupan, Anomaly free Froggatt-Nielsen models of flavor, J. High Energy Phys. 10 (2019) 188.
[24] M. Fedele, A. Mastroddi, and M. Valli, Minimal Froggatt-Nielsen textures, J. High Energy Phys. 03 (2021) 135.
[25] S. Nishimura, C. Miyao, and H. Otsuka, Exploring the flavor structure of quarks and leptons with reinforcement learning, J. High Energy Phys. 12 (2023) 021.
[26] D. Aloni, P. Asadi, Y. Nakai, M. Reece, and M. Suzuki, Spontaneous *CP* violation and horizontal symmetry in the MSSM: toward lepton flavor naturalness, J. High Energy Phys. 09 (2021) 031.

[27] D. Ringe, Probing intermediate scale Froggatt-Nielsen models at future gravitational wave observatories, Phys. Rev. D **107**, 015030 (2023).
[28] P. Asadi, A. Bhattacharya, K. Fraser, S. Homiller, and A. Parikh, Wrinkles in the Froggatt-Nielsen mechanism and flavorful new physics, J. High Energy Phys. 10 (2023) 069.
[29] Y.-C. Qiu, J.-W. Wang, and T. T. Yanagida, Predictions of m_{ee} and neutrino mass from a consistent Froggatt-Nielsen model, Phys. Rev. D **108**, 115021 (2023).
[30] C. Cornella, D. Curtin, E. T. Neil, and J. O. Thompson, Mapping and probing Froggatt-Nielsen solutions to the quark flavor puzzle, Phys. Rev. D **111**, 015042 (2025).
[31] S. Nishimura, C. Miyao, and H. Otsuka, Reinforcement learning-based statistical search strategy for an axion model from flavor, J. High Energy Phys. 10 (2025) 043.
[32] M. Ibe, S. Shirai, and K. Watanabe, Comprehensive bayesian exploration of Froggatt-Nielsen mechanism, J. High Energy Phys. 03 (2025) 150.
[33] S. Weinberg, Baryon- and lepton-nonconserving processes, Phys. Rev. Lett. **43**, 1566 (1979).
[34] P. Minkowski, $M \to e\gamma$ at a rate of one out of 10^9 muon decays?, Phys. Lett. **67B**, 421 (1977).
[35] T. Yanagida, Horizontal symmetry and masses of neutrinos, Prog. Theor. Phys. **64**, 1103 (1980).
[36] M. Gell-Mann, P. Ramond, and R. Slansky, Complex spinors and unified theories, Conf. Proc. C **790927**, 315 (1979).
[37] R. N. Mohapatra and G. Senjanović, Neutrino mass and spontaneous parity nonconservation, Phys. Rev. Lett. **44**, 912 (1980).
[38] See Supplemental Material at http://link.aps.org/supplemental/10.1103/c2ws-hx4h for technical details, generalizations, and supplemental plots, which also includes Refs. [39–61].
[39] I. M. Oldengott, G. Barenboim, S. Kahlen, J. Salvado, and D. J. Schwarz, How to relax the cosmological neutrino mass bound, J. Cosmol. Astropart. Phys. 04 (2019) 049.
[40] Z. Chacko, A. Dev, P. Du, V. Poulin, and Y. Tsai, Cosmological limits on the neutrino mass and lifetime, J. High Energy Phys. 04 (2020) 020.
[41] M. Escudero, T. Schwetz, and J. Terol-Calvo, A seesaw model for large neutrino masses in concordance with cosmology, J. High Energy Phys. 02 (2023) 142.
[42] Z.-z. Xing, H. Zhang, and S. Zhou, Impacts of the Higgs mass on vacuum stability, running fermion masses and two-body Higgs decays, Phys. Rev. D **86**, 013013 (2012).
[43] I. Esteban, M. Gonzalez-Garcia, M. Maltoni, T. Schwetz, and A. Zhou, The fate of hints: Updated global analysis of three-flavor neutrino oscillations, J. High Energy Phys. 09 (2020) 178.
[44] A. M. Baldini *et al.*, MEG upgrade proposal, arXiv:1301.7225.
[45] U. Bellgardt, G. Otter *et al.* (SINDRUM Collaboration), Search for the decay $\mu^+ \to e^+e^+e^-$, Nucl. Phys. **B299**, 1 (1988).
[46] A. Blondel *et al.*, Research Proposal for an experiment to search for the decay $\mu \to eee$, arXiv:1301.6113.
[47] B. Aubert *et al.* (*BABAR* Collaboration), Searches for lepton flavor violation in the decays $T^+ \to e^+\gamma$ and $\tau^+ \to M^+\gamma$, Phys. Rev. Lett. **104**, 021802 (2010).
[48] E. Kou, P. Urquijo *et al.* (Belle-II Collaboration), The Belle II physics book, Prog. Theor. Exp. Phys. **2019**, 123C01 (2019).
[49] K. Uno, K. Hayasaka *et al.* (Belle Collaboration), Search for lepton-flavor-violating tau-lepton decays to $\ell'\gamma$ at Belle, J. High Energy Phys. 10 (2021) 019.
[50] K. Hayasaka *et al.*, Search for lepton flavor violating Tau decays into three leptons with 719 million produced $\tau^+\tau^-$ pairs, Phys. Lett. B **687**, 139 (2010).
[51] P. Wintz, Results of the SINDRUM-II experiment, Conf. Proc. C **980420**, 534 (1998).
[52] W. Honecker *et al.* (SINDRUM II Collaboration), Improved limit on the branching ratio of μ-e conversion on lead, Phys. Rev. Lett. **76**, 200 (1996).
[53] B. Grzadkowski, M. Iskrzynski, M. Misiak, and J. Rosiek, Dimension-six terms in the standard model Lagrangian, J. High Energy Phys. 10 (2010) 085.
[54] M. Paraskevas, Dirac and Majorana Feynman rules with four-fermions, arXiv:1802.02657.
[55] M. Heikinheimo, K. Huitu, V. Keus, and N. Koivunen, Cosmological constraints on light flavons, J. High Energy Phys. 06 (2019) 065.
[56] C. Accettura *et al.*, Towards a muon collider, Eur. Phys. J. C **83**, 864 (2023).
[57] V. Shiltsev and F. Zimmermann, Modern and future colliders, Rev. Mod. Phys. **93**, 015006 (2021).
[58] Z. Chacko, N. Craig, P. J. Fox, and R. Harnik, Cosmology in mirror twin Higgs and neutrino masses, J. High Energy Phys. 07 (2017) 023.
[59] G. Alonso-Álvarez, D. Curtin, A. Rasovic, and Z. Yuan, Baryogenesis through asymmetric reheating in the mirror twin Higgs, J. High Energy Phys. 05 (2024) 069.
[60] A. Dedes, S. Rimmer, and J. Rosiek, Neutrino masses in the lepton number violating MSSM, J. High Energy Phys. 08 (2006) 005.
[61] E. Ma and U. Sarkar, Neutrino masses and leptogenesis with heavy Higgs triplets, Phys. Rev. Lett. **80**, 5716 (1998).
[62] M. Magg and C. Wetterich, Neutrino mass problem and gauge hierarchy, Phys. Lett. **94B**, 61 (1980).
[63] J. Schechter and J. W. F. Valle, Neutrino masses in SU(2) × U(1) theories, Phys. Rev. D **22**, 2227 (1980).
[64] G. Lazarides, Q. Shafi, and C. Wetterich, Proton lifetime and fermion masses in an SO(10) model, Nucl. Phys. **B181**, 287 (1981).
[65] R. N. Mohapatra and G. Senjanovic, Neutrino masses and mixings in gauge models with spontaneous parity violation, Phys. Rev. D **23**, 165 (1981).
[66] C. Wetterich, Neutrino masses and the scale of B-L violation, Nucl. Phys. **B187**, 343 (1981).
[67] D. M. Straub, FLAVIO: A Python package for flavour and precision phenomenology in the standard model and beyond, arXiv:1810.08132.

[68] J. Aebischer, J. Kumar, and D. M. Straub, WILSON: A Python package for the running and matching of Wilson coefficients above and below the electroweak scale, Eur. Phys. J. C **78**, 1026 (2018).

[69] A. M. Baldini *et al.* (MEG Collaboration), Search for the lepton flavour violating decay $M^+ \to e^+ \gamma$ with the full dataset of the MEG experiment, Eur. Phys. J. C **76**, 434 (2016).

[70] W. Bertl, R. Engfer *et al.* (SINDRUM II Collaboration), A search for μ-e conversion in muonic gold, Eur. Phys. J. C **47**, 337 (2006).

[71] L. Bartoszek, E. Barnes *et al.* (Mu2e Collaboration), Mu2e technical design report, arXiv:1501.05241.

[72] A. Aghamousa *et al.* (DESI Collaboration), The DESI experiment part I: Science, targeting, and survey design, arXiv:1611.00036.

[73] R. L. Workman *et al.* (Particle Data Group), Review of particle physics, Prog. Theor. Exp. Phys. **2022**, 083C01 (2022).

[74] M. Aker *et al.* (Katrin Collaboration), Direct neutrino-mass measurement based on 259 days of KATRIN data, Science **388**, adq9592 (2025).

[75] G. Adhikari *et al.* (nEXO Collaboration), NEXO: Neutrinoless double beta decay search beyond 10^{28} year half-life sensitivity, J. Phys. G **49**, 015104 (2021).

[76] A. Armatol, C. Augier *et al.* (CUPID Collaboration), Toward CUPID-1T, arXiv:2203.08386.

[77] C. Cornella, D. Curtin, G. Krnjaic, and M. Mellors, Testing the Froggatt-Nielsen mechanism with lepton violation, arXiv:2501.00629.